Desalination and Water Treatment
www.deswater.com

doi: 10.5004/dwt.2020.25378

185 (2020) 296–306
May

Fabrication of built in microfluidic systems for efficient electrochemical decolorization of reactive dyes

Zainab Mohammad Redha, Hayat Abdulla Yusuf*, Aysha Hamad AlGhatam

Department of Chemical Engineering, College of Engineering, University of Bahrain, P.O. Box: 32038, Manama, Bahrain, emails: hayousif@uob.edu.bh (H.A. Yusuf), Zali@uob.edu.bh (Z. Mohammad Redha), aysha103@hotmail.co.uk (A.H. Al Ghatam)

Received 14 July 2019: Accepted 19 December 2019

ABSTRACT

Textile wastewater is considered one of the most polluting effluents for ecosystems. Despite the various treatment methods used, its treatment still imposes a challenge on these industries especially with the increase in industrial activities. The electrochemical treatment of textile wastes has emerged as a promising solution, with almost no sludge production in comparison to other methods. In this paper, in house-fabricated electrochemical microfluidic systems were investigated for the electrochemical, indirect oxidation, decolorization of reactive dye solutions. Reactive Blue 19 and Reactive Yellow 181 dyes as single or mixed solutions were selected as models. Three effective electrochemical microfluidic chips designs were successfully fabricated: (1) a two-electrode cell (2E), (2) a three-electrode cell with reference electrode mounted on the top (3E-M), and (3) a three-electrode cell with an integrated reference electrode (3E-B). The electrochemical cells were characterized by their simple fabrication and effective performance. In all designs, 300 μm diameter carbon pencils were used as working and counter electrodes, along with an Ag/AgCl reference electrode. An experimental approach, using fractional factorial design, was used to study the optimum conditions for the degradation of each dye. The optimized factors were current density, pH, electrolyte concentration, dye concentration, and decolorization time. The percentage decolorization of the Reactive Blue was almost 100% in all of the microfluidic systems, while that of Reactive Yellow and the mixed solution were the highest in the 2E microfluidic chip, with efficiencies of 89% and 95%, respectively. Moreover, in optimum conditions, the performance of the three designs was investigated for the chemical oxygen demand (COD) removal in all dye solutions. Among the three designs, the 3E-M microfluidic chip was found to have the best capability for the COD removal, followed by 3E-M and then 3E-B. The reaction kinetics for the degradation process of each dye was found using the integrated method, and the results revealed pseudo-first-order reaction, with rate constants of 0.0545 and 0.0206 min^{-1} for Reactive Blue and Reactive Yellow, respectively.

Keywords: Electrochemical; Decolorization; Reactive Dye; Design of experiment; Miniaturization; Microfluidic systems

1. Introduction

There are pollutants in textile wastewaters such as organic load (starches, fats, waxes), color (dyes), sulfur, toxicants (heavy metals), salts, etc., which necessitate proper treatment before being discharged into water streams. Several techniques were used to treat textile wastewater, such as chemical oxidation methods, enzymatic methods, physico-chemical methods, microbiological treatments and electrochemical treatments [1,2]. Electrochemical methods of treatment proved to be effective in degrading non-biodegradable dyes such as reactive dyes and is considered one of the emerging techniques in the field [3]. Such methods were found to be cleaner than the chemical methods, since they

* Corresponding author.

This article was originally published with an error in one of the authors' name. This version has been corrected. Please see Corrigendum in vol. 186 (2020) 463 [10.5004/dwt.2020.26073].

don't produce any precipitates or sludge [4,5], in addition to their cost-effectiveness and efficient performance. Therefore, they have reached a well-recognized status nowadays [6–8].

1.1. Electrochemical treatment

Electrochemical textile wastewater treatments can be categorized as electrocoagulation, reduction, oxidation or electrochemical photo-assisted techniques. Electrochemical oxidation methods for decolorization of dye are based on generating hydroxyl radical species (M[OH•]), where M is the reactive dye that degrades by the following mechanism:

$$H_2O + M \rightarrow M\left[OH^{\bullet}\right] + H^+ + e^- \quad \text{(I)}$$

$$R + M\left[OH^{\bullet}\right] \rightarrow M + RO + H^+ + e^- \quad \text{(II)}$$

Indirect electrochemical oxidation is found as an effective technique for the decolorization of dyes. It is based on the formation of strong oxidants during electrolysis. There are two methods in this technique: one is using active chlorine and while the other is the electro-Fenton process. The use of active chlorine can be done by either gaseous chlorine, hypochlorous acid, or hypochlorite ions [6,7,9]. The reaction mechanism is given as follows:

$$2Cl^- \rightarrow Cl_{2(aq)} + 2e^- \quad \text{(III)}$$

$$Cl_{2(aq)} + H_2O \rightarrow ClO^- + Cl^- + H^+ \quad \text{(IV)}$$

$$M + ClO^- \rightarrow \text{Dye intermediates} \rightarrow CO_2 + H_2O + Cl^- \quad \text{(V)}$$

The main features of this method are that there is no solid waste generation, and there is no need for electrolyte addition since there are residual salts in industrial wastes [1]. The electro-Fenton process, on the other hand, occurs by the reaction of hydroxyl radicals from the hydrogen peroxide with the reactive dye in the presence of catalytic Fe^{2+} [10,11].

This paper focuses on the design and fabrication of three continuous microfluidic systems with two and three electrodes, for the decolorization of two reactive dye solutions: Reactive Yellow 181 (RY) and Reactive Blue 19 (RB) in single and multi-dye solutions. This is followed by the optimizing of the process variables for maximum decolorization efficiency using experimental design and the determination of the reaction kinetics for both dye solutions.

1.2. Microfluidic systems and miniaturized electrodes

Microfluidic systems offer promising abilities featured in manipulating the flow rate and optimizing the operating conditions, which are essential requirements for the presented application [12,13]. Moreover, miniaturized systems can provide additional benefits involving, large surface area to volume ratio, controlled mixing, and laminar flow properties leading to sufficient interaction time between reacted species, all of which result in increasing the reaction rate and subsequently developing the overall performance of the system [14,15]. In terms of industrial applications, micro-sizing the processes followed by numbering up could provide a better alternative to the conventional scaling-up of the industrial systems.

An Ag/AgCl reference electrode on a macroscale level can be fabricated as the conventional solid Ag/AgCl type or a pseudo-reference electrode where silver can either be electroplated, screen-printed, or deposited using chemical vapor deposition [16]. Miniaturization of the Ag/AgCl reference electrode took difference forms such as a Needle-Type Ultra Micro Ag/AgCl electrode [17] or as a micro capillary where AgCl was deposited on an Ag wire in the capillary or using a barrel pen, which showed a good level of stability and repeatability [18].

2. Fabrication

Three continuous electrochemical microfluidic systems were constructed: a two-electrode microfluidic chip, a three-electrode microfluidic chip with a mounted miniaturized Ag/AgCl reference electrode, and a three-electrode microfluidic chip with a built-in liquid Ag/AgCl reference electrode. They were all fabricated on a 3 cm × 8 cm × 0.6 mm clear acrylic substrate. The channels were done using CNC milling machining (DATRON Technology Ltd., Milton Keynes, UK). However, constructing the electrodes, wiring, soldering, and miniaturizing the Ag/AgCl reference electrode were done manually in-house. 300 μm diameter carbon pencils were used as electrodes (Hi-Polymer 2180 B, LYRA™ Orlow Techno®). All electrodes were stored away from direct sunlight, at a room temperature of 26°C–28°C.

2.1. Two-electrode microfluidic chip (2E)

For the construction of the 2E microfluidic chip, first, the two electrodes were adjusted within the channel and secured with clear epoxy glue on each side. The active length of the working electrode is 2 cm. The active side of the counter electrode is only 300 μm of the diameter while the rest is insulated with epoxy glue. This resulted in an area of the electrodes of 11.9 mm^2. Then, a lamination sheet was used to seal the channel at 120°C, and the connecting wire then soldered. In order to secure the solder and the laminating paper, the chip was then coated with a thin layer of clear epoxy glue. The final constructed 2E-Chip has a capacity of 61.5 mm^2 and is illustrated in Fig. 1

2.2. Miniaturized Ag/AgCl reference electrode

A miniaturized Ag/AgCl reference electrode was constructed using an l5 mL clear plastic syringe. The syringe was filled with 1 mL of liquefied 2% agar in 3.33 M KCl, then, when solidified, 3.33 M of KCl was filled to the top of the syringe. The syringe cap has a 1 mm hole for the Ag wire to be placed in and the Ag wire is 0.5 mm diameter-925 carat silver.

The reference electrode was first washed in distilled water and then immersed in 7% sodium hypochlorite for an hour. This was followed by washing it again with distilled water then drying and putting 3.33 M KCl within the syringe. Finally, the syringe was closed carefully to avoid having any

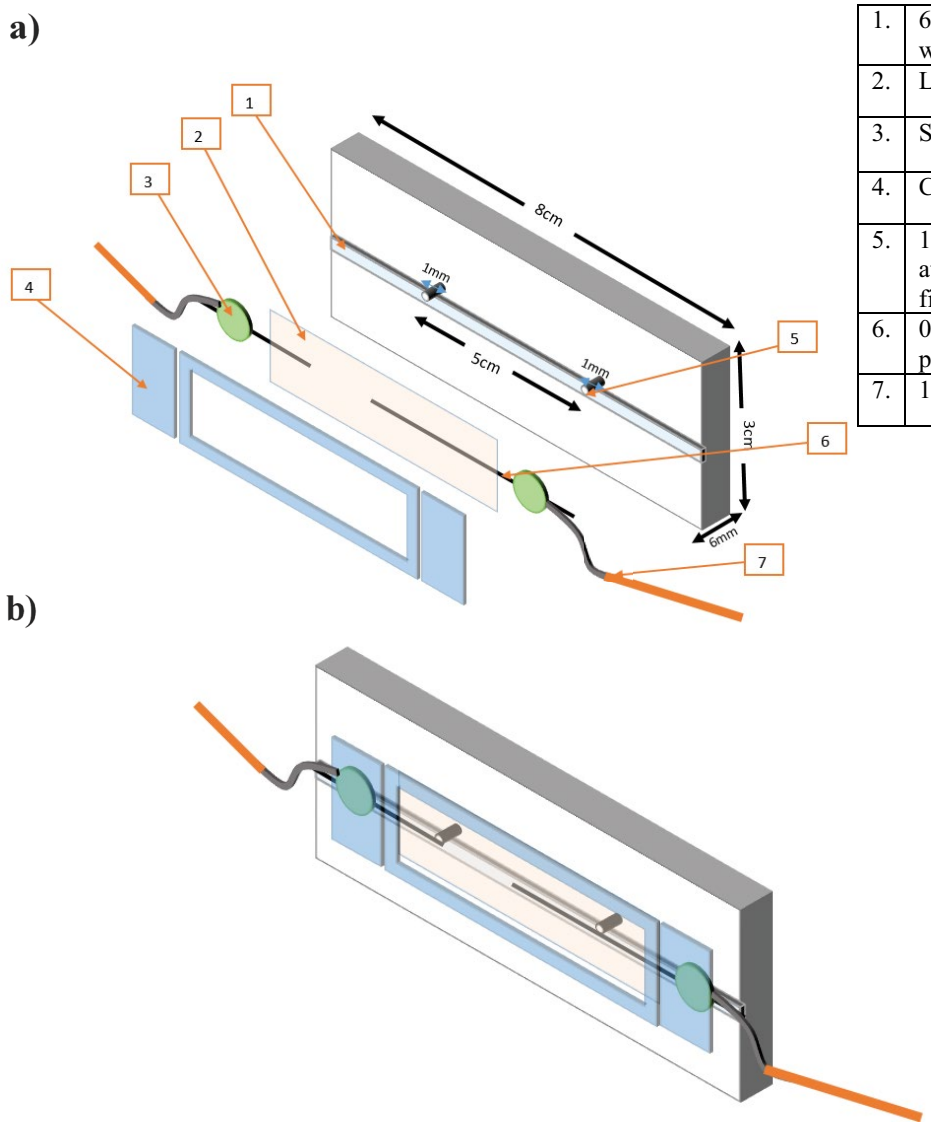

1.	600 µm depth x 2mm width flow channel
2.	Lamination sheet
3.	Solder
4.	Clear Epoxy glue
5.	1mm diameter hole attached to 1mm plastic fitting
6.	0.3mm diameter carbon pencil
7.	1mm wire

Fig. 1. Two electrodes microfluidic systems (2E-Chip): (a) Layers and the chip components and (b) assembled chip (2E).

air bubbles and the Ag wire secured in place with a small amount of epoxy on the top of the syringe cap. A schematic diagram of the electrode is shown in Fig. 2.

2.3. Three electrodes microfluidic system with the miniaturized Ag/AgCl reference electrode mounted (3E-M Chip)

The three electrodes cell consists of three holes: two are considered as the inlet and outlet, while the middle 2 mm hole is used to mount the miniaturized Ag/AgCl electrode. The middle 2 mm hole was first filled with 2% agar in 3.33 M KCl hot liquid where after waiting to set, it was trimmed to fit the reference electrode. The 2mm hole was then topped with filter paper and secured in place. After that, the same 2E fabrication process was followed here for the electrode assembling, and both laminating and soldering of the wires. The final microfluidic system is shown in Fig. 3. The active area of the electrodes in this design is 38.3 mm^2, and the fluid volume is 58.5 mm^3.

2.4. Three electrodes microfluidic system with a built-in Ag/AgCl reference electrode (3E-M)

The fabrication of the three electrodes with the Ag/AgCl reference electrode built into the microfluidic system was done by first making a flow channel of 5 mm in length and 1 mm width. This 1mm stream channel was bridged with the KCl reference electrode channel, as shown in Fig. 4. It was then sanded to avoid any roughness in the channel and filled with a hot 2% agar in 3.33 M KCl liquid, where the filter paper was put into the channel before the agar solidifies. After the solidification took place, a small layer of epoxy glue was put on top of the small constructed channel without blocking either side of the main channels. Then the electrodes were assembled into the cell in the same way as in the fabrication process of the two-electrode microfluidic system. It was then sealed with a lamination sheet. An AgCl electrode was made in the same way as in the fabrication process of the miniaturized Ag/AgCl reference electrode and Epoxy glue and a cap

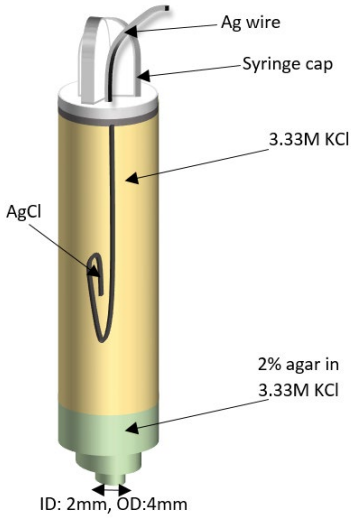

Fig. 2. Miniaturized Ag/AgCl reference electrode.

were applied in order to secure any leaking from the built-in reference electrode. The fluid volume in this microfluidic system is 28.372 mm^3, with electrodes having an active area of 52.44 mm^2. The final assembled microfluidic system is shown in Fig. 4.

3. Experimental work

3.1. Reagents

The chemicals used in this study were: hydrochloric acid (37 wt.%, ACS, ISO from Scharlau, Barcelona, Spain), sodium hydroxide (Timstar Laboratory Suppliers Ltd., Cheshire, UK), Reactive Blue 19 (Town End Plc., Leeds, UK), Reactive Yellow 181 (Ciba Specialty Chemicals, Basel, Switzerland), sodium chloride (Research-Lab fine Chem industries, Maharashtra, India), potassium chloride (Scharlau, Barcelona, Spain), sodium hypochlorite (5.25 wt. %, Scharlau, Barcelona, Spain), agar flakes (Clear Spring).

3.2. Apparatus

The main equipment used in this study were potentiostat (EZstat-pro), ATCO Weighing scale (Model no. AB1-009 F410AB0041-W-LTO4), pH meter (Metrohm 780), UV-Spectrophotometer (UV-1800, Shimadzu, Kyoto, Japan), variable flow pump (Model: 73160-05, Cole-Parmer, Maharashtra, India), filter paper (Hollingsworth & Vose company LTD, East Walpole, UK), 1,000 µL Micropipette (Eppendorf Reference® Hamburg, Germany).

3.3. Experimental setup and procedure

3.3.1. Calibration of the miniaturized Ag/AgCl reference electrode

The Ag/AgCl Reference Electrode was calibrated by the difference of the voltage between the miniaturized Ag/AgCl reference electrode and the Metrohnm Ag/AgCl in a conducting solution of 20 ppm RY and an electrolyte of 12 g/L sodium chloride. The voltage difference is measured at 0.003 V with the 5 mL miniaturized Ag/AgCl reference electrode and 0.0017 V with the 10 mL miniaturized Ag/AgCl reference electrode.The batch and continuous experimental setups and procedures are illustrated as follows:

3.3.2. Batch experiment

For the batch experiment, 300 µm diameter carbon pencils are used as the working and counter electrodes, and the

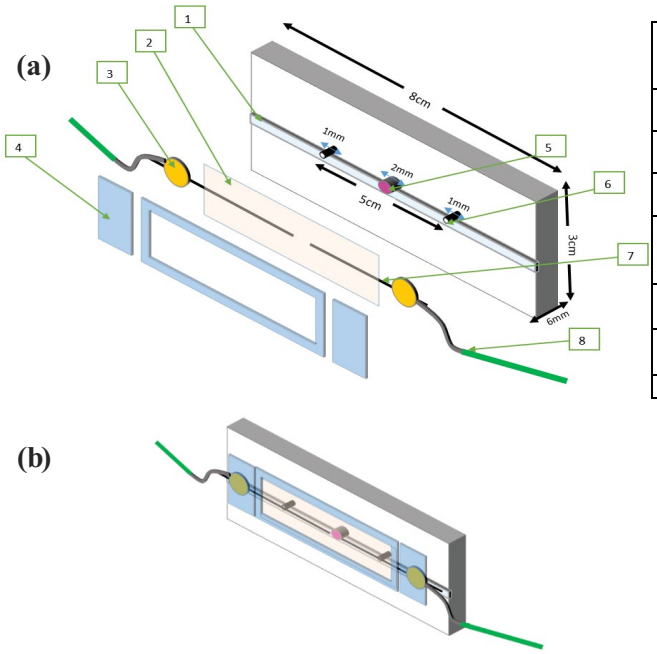

1.	600 µm depth x 2mm width flow channel
2.	Lamination sheet
3.	Solder
4.	Clear epoxy glue
5.	2mm hole with 2% agar in 3.33M KCl and filter paper and 2mm plastic fitting
6.	1mm diameter hole attached to 1mm plastic fitting
7.	0.3mm diameter carbon pencil
8.	1mm wire

Fig. 3. Three electrodes microfluidic system (3E-M Chip): (a) Layers and the chip components and (b) assembled chip.

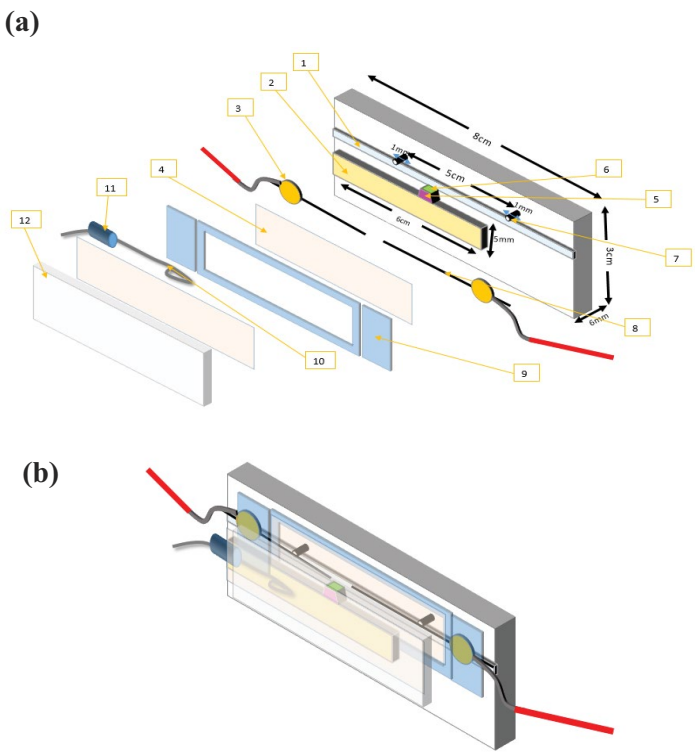

1.	600 µm depth x 2mm width flow channel
2.	3mm depth x 3mm width reference electrode channel filled with 3.33M KCl
3.	Solder
4.	Lamination sheet
5.	2 %agar in 3.33M KCl
6.	Filter paper
7.	1mm diameter hole attached to 1mm plastic fitting
8.	0.3mm diameter carbon pencil
9.	Clear epoxy glue
10.	Ag/AgCl
11.	Tube
12.	7cm length x 2cm width x0.2mm thickness clear plastic

Fig. 4. Three electrodes microfluidic system (3E-B Chip) with a built-in liquid Ag/AgCl reference electrode: (a) Layers and the chip components and (b) assembled chip (3E-B).

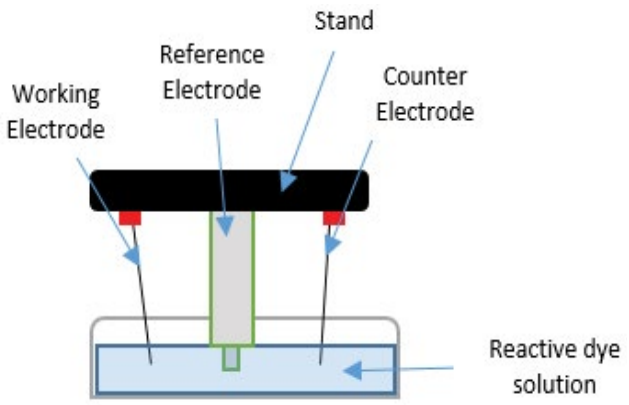

Fig. 5. Batch experiment setup.

Ag/AgCl Metrohnm is used as the reference electrode, as illustrated in Fig. 5.

The batch experiments were utilized to (1) tackle the electrode deposition problem faced in a previous study [19], (2) optimize the operating conditions for each dye and for the mixture of the dyes, and (3) study kinetics of the reaction and the decolorization rate accordingly.

3.3.3. Continuous experiments

Three continuous microfluidic system setups (one per chip) were used, as illustrated in Fig. 6.

For each dye; RB 19 and RY 181, two-level fractional factorial design with 16 experiments per dye was constructed. The investigated factors are degradation of time, pH, NaCl concentration, dye concentration, and current density. The measured response was decolorization efficiency. The low and high levels are shown in Table 1.

For the mixture dye experiments, the factors that are similar to the single dye experiments have not been changed while the pH, Reactive Yellow concentration, and Reactive Blue concentration were considered in this optimization process. Therefore, Box–Behnken design has been chosen, following several researches in the literature [21,22]. The constructed experiments were 15 with the three levels as shown in Table 2. The NaCl concentration was 12 g/L with a running time of 10 min and a current density of 0.002 A/cm^2, as detailed in section 5.3. All experiments were run at room temperature with a constant volume of 20 mL

3.3.4. %chemical oxygen demand removal

The % chemical oxygen demand (COD) of the degraded solutions was tested in the three fabricated chips: 2E, 3E-M, and 3E-B, at the optimum operating conditions. The COD reduction was calculated using the following Eq. (1) [23]:

$$\%\mathrm{COD}_{\mathrm{reduction}} = \frac{\mathrm{COD}_i - \mathrm{COD}_f}{\mathrm{COD}_i} \times 100 \quad (1)$$

where COD_i and COD_f are the chemical oxygen demand of the pre- and post-treated effluent, respectively.

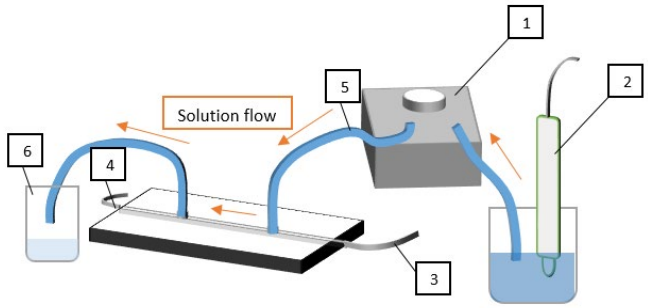

1.	Peristaltic pump
2.	Ag/AgCl Reference Electrode
3.	Working Electrode connection
4.	Counter electrode connection
5.	1mm diameter acrylic tubes
6.	Outlet beaker

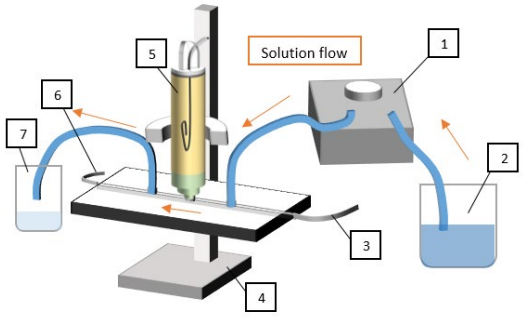

1.	Peristaltic pump
2.	Inlet Solution Glass Beaker
3.	Working Electrode connection
4.	Stand
5.	Miniaturized Ag/AgCl Reference Electrode
6.	Counter Electrode connection
7.	Outlet Glass Beaker

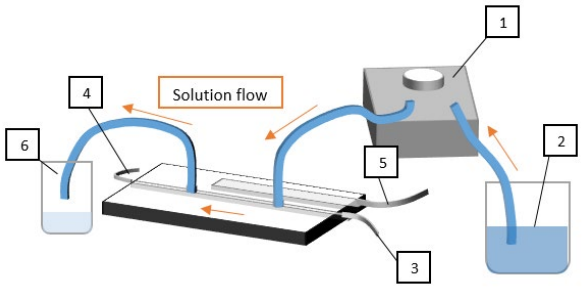

1.	Peristaltic pump
2.	Inlet Solution Glass Beaker
3.	Built in Ag/AgCl Reference Electrode
4.	Working Electrode connection
5.	Counter Electrode connection
6.	Outlet solution Glass Beaker

Fig. 6. Experimental setup for (a) 2E-Chip, (b) 3E-M Chip, and (c) 3E-B Chip.

Table 1
Levels for the fractional factorial design of experiment for single dyes

Level/factor	–1	1
Time (min)	5	10
pH	3	10
$[NaCl]_i$ (g/L)	6	12
$[Dye]_i$ (ppm)	20	50
Current density (A/cm^2)	0.002	0.003

Table 2
Levels for the Box–Behnken design for the mixture dye experiments

Level/Factor	pH	$[RB]_i$ (ppm)	$[RY]_i$ (ppm)
–1	3	20	20
0	7	35	35
1	10	50	50

4. Results and discussion

4.1. Calibration curves

The calibration curve for Reactive Blue 19 (λ = 596 nm) and for Reactive Yellow 181 (λ = 410 nm) are given in Figs. 7 and 8, respectively. A linear relationship between absorbance and concentration was obtained in agreement with Beer Lambert's law, as presented in the graphs.

4.2. Batch experiment results

The decolorization efficiency results at different operating conditions, for the single dye and mixed solutions, were analyzed using Minitab®. The decolorization efficiency was found using the following Eq. (2):

$$\text{Decolorization efficiency} = \frac{\left(\text{Absorbance}_i - \text{Absorbance}_f\right)}{\text{Absorbance}_i} \times 100 \quad (2)$$

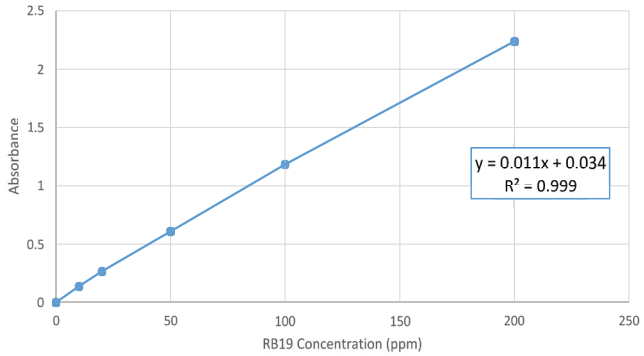

Fig. 7. Calibration curve for Reactive Blue.

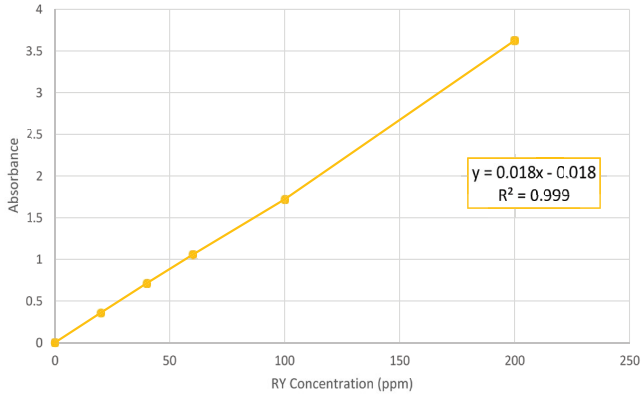

Fig. 8. Calibration curve for Reactive Yellow.

where the subscripts '*i*' and '*f*' stand for the initial and final conditions, respectively.

4.2.1. Reactive Blue 19

The Pareto Chart and Normal Plot of the effects of the different factors and their interactions for the Reactive Blue 19 solution are shown in Figs. 9 and 10, respectively. Both plots agree that the most significant factor is the dye concentration. The following predominant factors are the electrolyte concentration and the running time, as illustrated in Figs. 9 and 10 indicate the direction of the effect. It shows a significant negative standardized effect for the concentration in comparison to all other insignificant effects.

After eliminating the insignificant factors, the Reactive Blue response equation from Minitab was found as:

$$\text{Response} = 7.295 - 3.361\left(\text{Conc}_i\right) \quad (3)$$

Fig. 11 shows the effects plot for the Reactive Blue decolorization process. The decolorization was directly proportional to time and electrolyte concentration, while it was inversely proportional to the dye concentration and pH. Accordingly, it was found that better decolorization was achieved in acidic environments [24], and in terms of the electrolyte concentration, it was found that the higher the concentration of electrolyte, the better the decolorization efficiency. However,

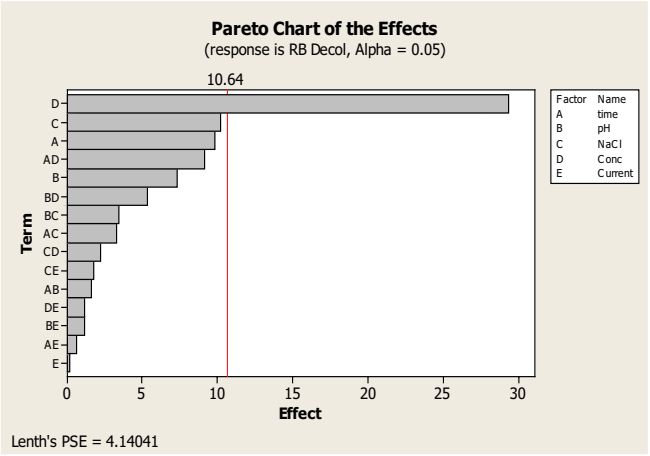

Fig. 9. Pareto chart of Reactive Blue.

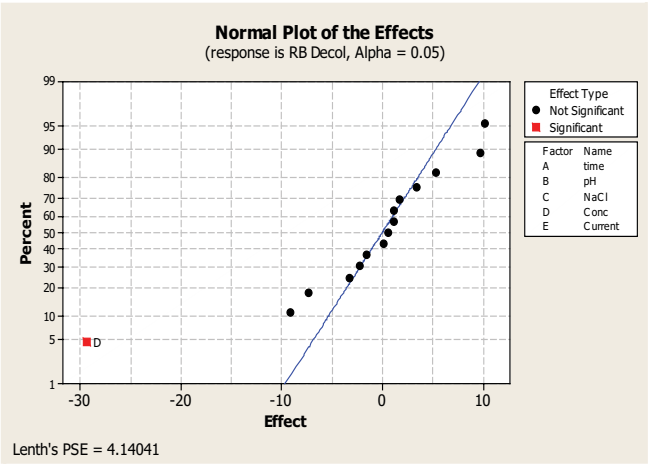

Fig. 10. Normal plot of effects for Reactive Blue.

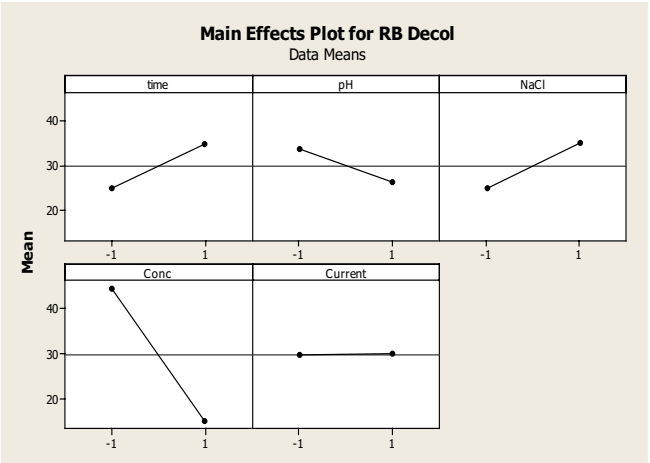

Fig. 11. Effects plot for Reactive Blue decolorization.

changing the current density did not provide any significant effect on the decolorization response as shown in Fig. 11. The figure also revealed that longer reaction time is better for achieving higher decolorization efficiency.

In addition, the analysis of the results showed that the best decolorization efficiency was 64.03% at the following operating conditions: time = 10 min, pH 3, 12 g/L electrolyte concentration, 20 ppm initial concentration of Reactive Blue and a current density of 0.003 A/cm^2.

4.2.2. Reactive Yellow 181

Similarly, the factors and their interactions were also analyzed for Reactive Yellow dye. A Pareto Chart and Normal Plots of the effects are shown in Figs. 12 and 13, respectively. The most significant factor was found to be the concentration of the dye. The second highest factor affecting the decolorization was the reaction time. Fig. 13 reveals a negative standardized effect for the concentration relative to the effect of other factors, but with a lower level in comparison to that obtained with RB.

After eliminating the insignificant factors, Minitab gives the following response equation for Reactive Yellow 181:

$$\text{Response} = 7.295 - 3.361\left(\text{Conc}_i\right) \quad (4)$$

Fig. 14 shows directly proportional relationships between the decolorization and both time and electrolyte concentration, while it was inversely proportional to the dye concentration and pH. The best decolorization efficiency was 19.54% at the following operating conditions: time = 10 min, pH 10, 12 g/L electrolyte concentration, 20 ppm initial concentration of Reactive Blue, and a current density of 0.002 A/cm^2.

4.2.3. Mixture of dyes

Analyzing the absorbance spectrum for the mixture revealed two peaks. The high wavelength peak (λ_{max} = 596 nm) represents Reactive Blue dye in the solution, while the low wavelength peak (λ_{max} = 410 nm) represents the Reactive Yellow dye in the solution. Therefore, two responses were measured: decolorization for the RB and RY in the mixture solution, in Figs. 15 and 16, respectively.

The main effects plots illustrate the effects of varying each parameter on the measured response. For example, pH and the type of dye (RB in Fig. 15, and RY in Fig. 16) had the biggest impact on the measured response. In particular, Fig. 15 shows clearly that RY has minimal effect on the RB decolorization in the mixed solution, within the selected range of values since it has the least steep line with the response. One the other hand, all factors show an almost similar effect for RY decolorization in Fig. 16. The optimum operating conditions for the decolorization of both RB and RY in the mixed solution were found using Minitab to be pH 3, reactive dye concentration of 20 ppm, and Reactive Yellow concentration of 20 ppm, as well.

The optimized conditions are summarized in Table 3.

4.3. Continuous experiment results

The three microfluidic systems were operated at optimum conditions found from the batch experiments. All experiments were performed with an inlet flow rate of 0.1 mL/min, and all readings were taken at a wavelength of 594 nm for the blue color, and 410 nm for the yellow color. The decolorization efficiency was calculated for all the

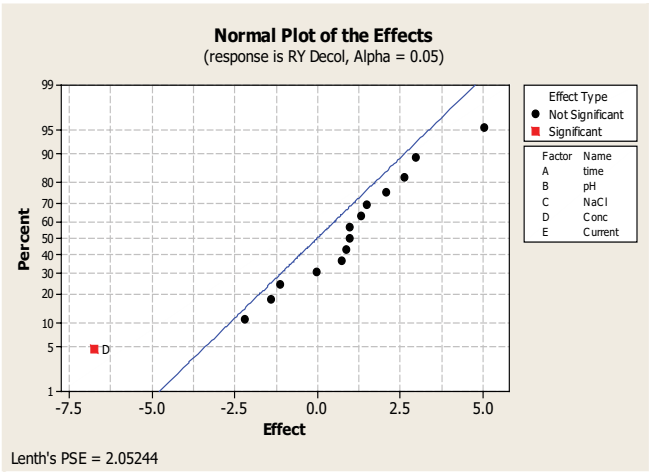

Fig. 13. Normal Plot for the effects study in Reactive Yellow decolorization.

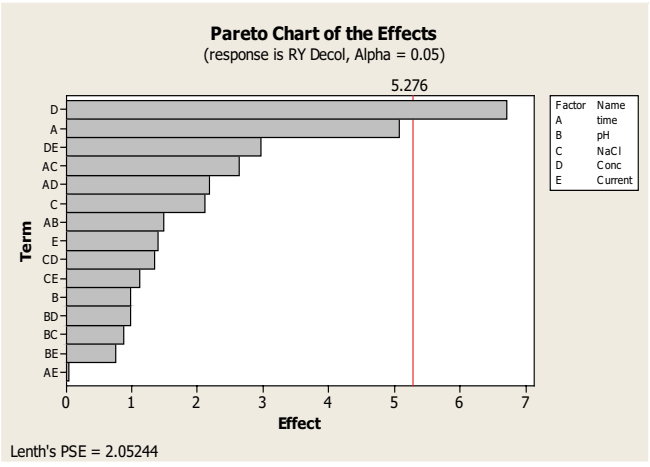

Fig. 12. Pareto chart for the effects study in Reactive Yellow decolorization.

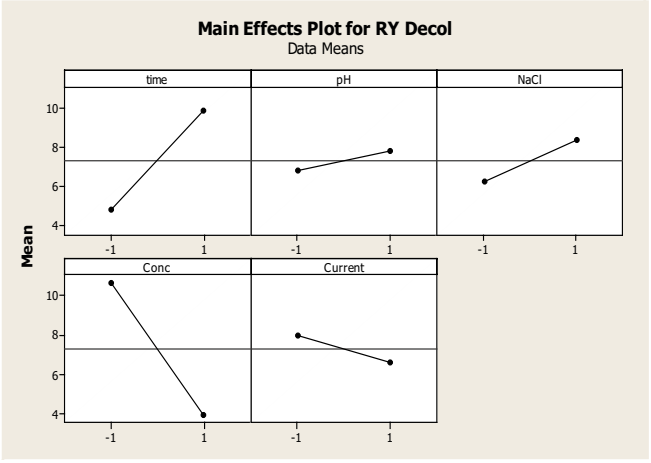

Fig. 14. Main effects plot for Reactive Yellow decolorization.

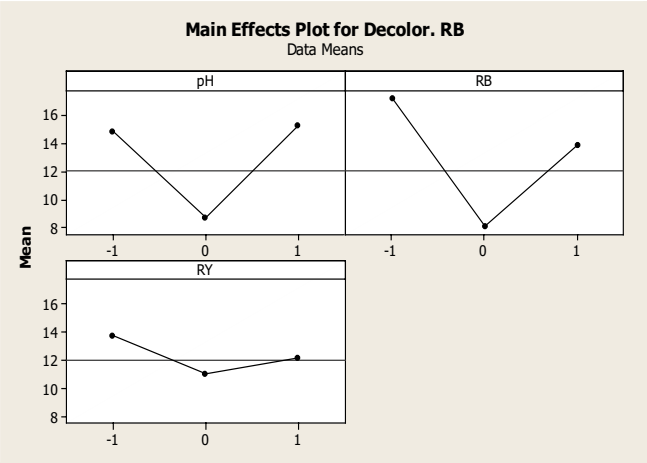

Fig. 15. Main effects plot for the mixed solution - blue decolorization.

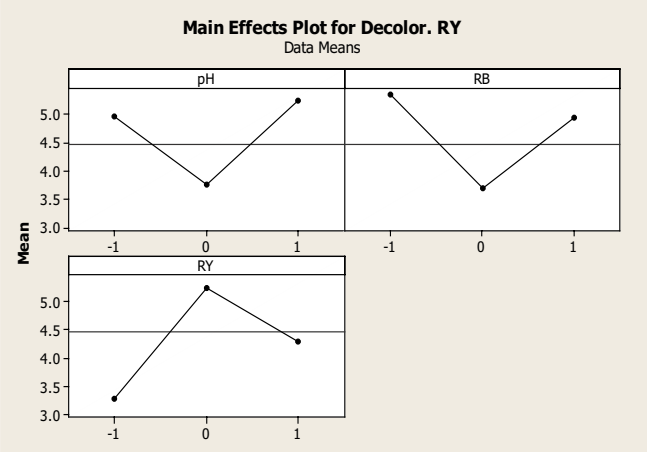

Fig. 16. Main effects plot for the mixture solution - yellow decolorization.

Table 3
Summary of the optimized conditions

Factors	Reactive Blue	Reactive Yellow	Mixture
pH	3	10	3
$[NaCl]_i$ (g/L)	12	12	12
$[RB]_i$ (ppm)	20	0	20
$[RY]_i$ (ppm)	0	20	20
Time (min)	10	10	10
Current (A/cm^2)	0.002	0.002	0.002

microfluidic systems using Eq. (1) and the results are illustrated in Fig. 17.

All fabricated microfluidic devices gave 100% RB decolorization. The RY %decolorization was highest with the 2E-chip, which was 89%, while it was 75%, and 55% with 3E-M and 3E-B, respectively.

For the mixed solution, the blue color decolorization was very high. It was around 95% with 2E and 93%

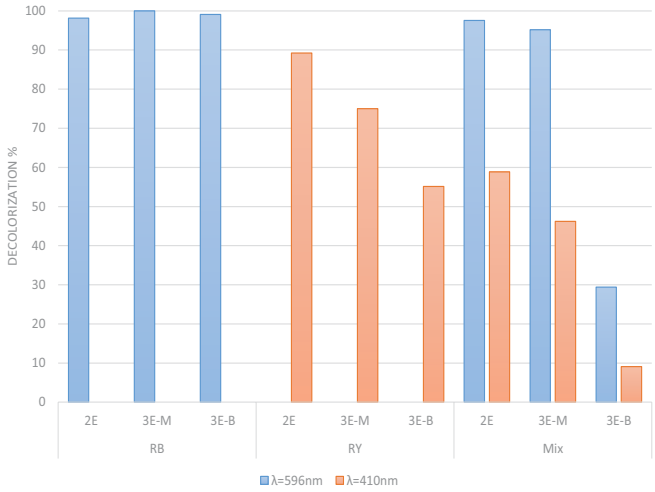

Fig. 17. Decolorization efficiency in the three fabricated microfluidic systems, at optimized conditions.

with 3E-M, while it was 30% with 3E-B. The yellow color decolorization was lower than the blue one as the highest decolorization efficiency was 60% with the 2E chip, 45% with 3E-M, and 10% with 3E-B. It should be noted that there was electrodeposition on the working electrode of 3E-B and 3E-M when Reactive Yellow and the mixed solution were used. The electrodeposition mainly occurs due to the constructed reference electrode, especially when increasing the current density. In addition, a few instances of electrode instability caused some fluctuation in the voltage of the cell provided by the counter electrode.

Reactive Blue decolorization was high in all of the fabricated microfluidic systems, while the decolorization efficiency of the Reactive Yellow and the mixture varied in each design. The highest level of efficiency was achieved in the microfluidic chip 2E, the lowest in 3E-B. This reduction in the decolorization efficiency could be attributed to the close proximity of the reference electrode in 3E chips in comparison to 2E as argued in the study conducted by Zhang et al. [25]. In addition, the working electrode placement was found to be of crucial consideration in designing the electrochemical cell. Accordingly, it was found that moving the working electrode as close as possible to the reference electrode reduced the Ohmic drop. This can be done by a Luggin-capillary. It was also observed that there was electrodeposition on the working electrode in the 3E-B and 3E-M when Reactive Yellow and the mixed solution were used, which subsequently affected the rate of decolorization.

In summary, the decolorization of RB 19 was investigated by many researchers, using different techniques. Recent studies, using the coagulation treatment method, reported 69% [26] and 68% [27] decolorization of the RB 19 dye. A range of 96%–100% decolorization of this dye was reached using photocatalytic and photochemical degradation techniques [11,28,29]. Other researchers showed almost complete decolorization using advanced biological treatment methods [30]. However, to the authors' knowledge, the only recorded data on the electrochemical decolorization of RB 19 was presented recently in a review paper [31].

The review reported that decolorization percent as high as 90% was reached using electrochemical advanced oxidation processes [32]. This indicates that the electrochemical decolorization method investigated in the current study outweighs the other method as 100% decolorization was successfully achieved for RB 19 in all fabricated microfluidic devices.

Concerning RY 181 dye, decolorization studies on this dye, in particular, seemed to be very limited [33]. A recent study done by the same group achieved 92.9% decolorization of the same dye using the Fenton oxidation method [33]. However, there are few studies on other types of Reactive Yellow dyes. For example, in a study on RY 14 dye, it was reported that with advance oxidation processes, a decolorization of 91% could be achieved [34]. On the other hand, with electrochemical methods, 89% decolorization was successfully achieved in the current paper using the 2 E chip for RY 181, in comparison to 80% decolorization reported using the same technique for a similar Reactive Yellow dye name RY 160 [35]. Therefore, this work presents better results over other electrochemical decolorization methods of Reactive Yellow dyes.

4.4. %COD removal

Using Eq. (1) in section 4.3.4, it was found that the 3E-M microfluidic chip had the best capability for COD removal in all prepared dye solutions, followed by the 2E then 3E-B microfluidic chips. The best COD reduction was found to be 76%, 64%, and 45% in RB, RY, and mixed solutions respectively, calculated at the optimum operating conditions, as shown in Fig. 18

4.5. Reaction kinetics

In order to determine the reaction rate, an isolation method was used, where the reactants are kept in large quantities, then the rate of the reaction was approximated [36]. It was found that the best representation for the reaction

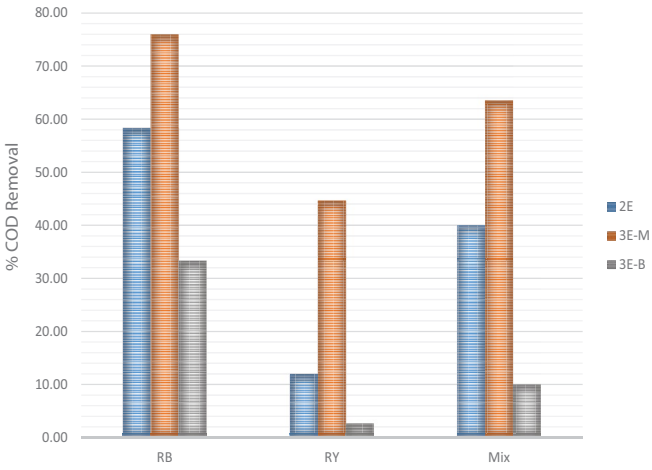

Fig. 18. %COD reduction in the three microfluidic systems, at the optimum operating condition of the RB solution, RY solution, and mixture solution of RB and RY.

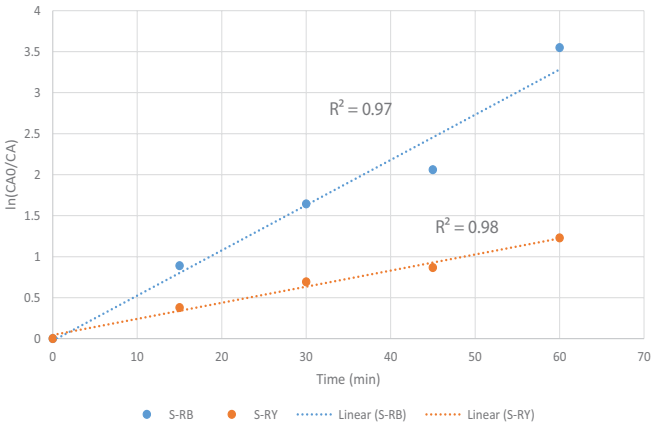

Fig. 19. First-order reaction kinetics of the electrochemical degradation of Reactive Blue and Reactive Yellow dyes in the 3E-M fabricated microfluidic system.

kinetics was pseudo-first-order, with R^2 = 0.97 and 0.99 with Reactive Blue and Reactive Yellow, respectively, as presented in Fig. 19. The calculated rate constants were found to be 0.0545 and 0.0206 min^{-1} for Reactive Blue and Reactive Yellow, respectively. The following rate of reaction expressions was used:

$$-r_A = kC_A \tag{5}$$

where k is rate constant and C_A is Concentration of the dye, A, and the integration form is as follows:

$$\ln\frac{C_{A0}}{C_A} = kt \tag{6}$$

5. Conclusion

All fabricated microfluidic chips showed promising results for the presented application. Three electrochemical microfluidic systems were constructed: a two-electrode cell, a three-electrode cell with a constructed reference electrode, mounted on top (3E-M) and a three-electrode cell with a reference electrode incorporated within the cell (3E-B). High Decolorization efficiency of single and mixture of Reactive Blue 19 and Reactive Yellow 181 was achieved using the fabricated electrochemical microfluidic systems. This is extremely advantageous for textile effluent treatment, where there are no sludge residues, compared to chemical decolorization, commonly used in the industry. The efficient decolorization process in these designs was mainly attributed to the unique features offered by miniaturization. The decolorization was almost 100% with RB in all of the microfluidic systems. The best RY and mixed solution decolorization were 89% with 95% with the 2E chip. The 3E-M chip was found to give the best COD removal in all prepared dye solutions, followed by 3E-M then 3E-B. Finally, the reaction kinetics for the degradation process of each dye was found as pseudo-first-order. Further studies can be made on the reaction kinetics and interaction effect in mixed solutions of both dyes.

References

[1] G.A.R. Oliveira, E.R.A. Ferraz, F.M.D. Chequer, M.D. Grando, J.P.F. Angeli, M.S. Tsuboy, J.C. Marcarini, M.S. Mantovani, M.E. Osugi, T.M. Lizier, M.V.B. Zanoni, D.P. Oliveira, Chlorination treatment of aqueous samples reduces, but does not eliminate, the mutagenic effect of the azo dyes Disperse Red 1, Disperse Red 13 and Disperse Orange 1, Mutat. Res. Genet. Toxicol. Environ. Mutagen., 703 (2010) 200–208.

[2] C.A. Martínez-Huitle, E. Brillas, Decontamination of wastewaters containing synthetic organic dyes by electrochemical methods: a general review, Appl. Catal., B, 87 (2009) 105–145.

[3] C.A. Martínez-Huitle, S. Ferroa, Electrochemical oxidation of organic pollutants for the wastewater treatment: direct and indirect processes, Chem. Soc. Rev., 35 (2006) 1324–1340.

[4] P.V. Nidheesh, G. Divyapriya, N. Oturan, C. Trellu, M.A. Oturan, Environmental applications of boron-doped diamond electrodes: 1. Applications in water and wastewater treatment, ChemElectroChem, 6 (2019) 2124–2142.

[5] F. Orts, A.I. del Río, J. Molina, J. Bonastre, F. Cases, Study of the reuse of industrial wastewater after electrochemical treatment of textile effluents without external addition of chloride, Int. J. Electrochem. Sci., 14 (2019) 1733–1750.

[6] M. Sala, C. Gutierraz-Bouzan, Electrochemical techniques in textile processes and wastewater treatment, Int. J. Photoenergy, 2012 (2012) 1–12, https://doi.org/10.1155/2012/629103.

[7] L.H. Sheng, C.F. Peng, Treatment of textile wastewater by electrochemical method, Water Res, 28 (1994) 277–282.

[8] C.A. Martínez-Huitle, M. Panizza, Electrochemical oxidation of organic pollutants for wastewater treatment, Curr. Opin. Electrochem., 11 (2018) 62–71.

[9] A.B.M. Panizza, R. Ricotti, G. Cerisola, Electrochemical degradation of methylene blue, Sep. Purif. Technol., 54 (2007) 382–387.

[10] N. Daneshvar, S. Abe, V. Vatanpour, M.H. Rasoulifard, Electro-Fenton treatment of dye solution containing Orange II: influence of operational parameters, J. Electroanal. Chem., 615 (2008) 165–174.

[11] H.A. Yusuf, Z.M. Redha, A.J. Al Meshal, H.J. Shehab, Experimental and mathematical modelling of reactive dyes decolorization using fenton oxidation process in a microfluidic system, Desal. Water Treat, 116 (2018) 305–316.

[12] N. Wang, X. Zhang, Y. Wang, W. Yu, H.L.W. Chan, Microfluidic reactors for photocatalytic water purification, RSC Adv., 14 (2013) 1074–1082.

[13] Z. Mohammed Redha, H. Abdulla Yusuf, H.A. Ahmed, P.R. Fielden, N.J. Goddard, S.J. Baldock, A miniaturized injection-moulded flow-cell with integrated conducting polymer electrodes for on-line electrochemical degradation of azo dye solutions, Microelectron. Eng., 169 (2017) 16–23.

[14] N.-T. Nguyen, S.T. Wereley, Fundementals and Applications of Microfluidics, Artech House, Inc., Norwood, 2006.

[15] H.A. Yusuf, Z.M. Redha, S.J. Baldock, P.R. Fielden, N.J. Goddard, An analytical study of the electrochemical degradation of methyl orange using a novel polymer disk electrode, Microelectron. Eng., 149 (2016) 31–36.

[16] M.W. Shinwari, D. Zhitomirsky, I.A. Deen, P.R. Selvanapathy, M.J. Deen, D. Landheer, Microfabricated reference electrodes and their biosensing applications, Sensors, 10 (2010) 1679–1715.

[17] T. Kitade, K. Kitamura, S. Takegami, Y. Miyata, M. Nagatomo, T. Sakaguchi, M. Furukawa, Microfabricated reference electrodes and their biosensing applications, Anal. Sci., 21 (2005) 907–912.

[18] S. Inamdar, M. Bhat, S. Haram, Construction of Ag/AgCl reference electrode from used felt-tipped pen barrel for undergraduate laboratory, J. Chem. Educ., 86 (2009) 355–356.

[19] A.J. AlMeshal, H.J. Shehab, Implementation of Microfluidic Systems in Reactive Dyes Decolorization Using Fenton's Oxidation and Electrochemical Oxidation Process, Senior Project, Kingdom of Bahrain, 2015, pp. 20–55.

[20] K. Oukili, M. Loukili, Optimization of textile azo dye degradation by electrochemical oxidation using Box–Behnken design, Mediterr. J. Chem., 8 (2019) 410–419.

[21] N.C. Fernandes, L.B. Brito, G.G. Costa, S.F. Taveira, M.S.S. Cunha–Filho, G.A.R. Oliveira, R.N. Marreto, Removal of azo dye using Fenton and Fenton-like processes: Evaluation of process factors by Box–Behnken design and ecotoxicity tests, Chem. Biol. Interact., 291 (2018) 47–54.

[22] P. Kaur, V.K. Sangal, J.P. Kushwaha, Parametric study of electro-Fenton treatment for real textile wastewater, disposal study and its cost analysis, Int. J. Environ. Sci. Technol., 16 (2019) 801–810.

[23] S.S. Vaghela, A.D. Jethva, B.B. Mehta, S.P. Dave, S. Adimurthy, G. Ramachandraiah, Laboratory studies of electrochemical treatment of industrial azo dye effluent, Environ. Sci. Technol., 39 (2005) 2848–2855.

[24] S. Karthikeyan, A. Titus, A. Gnanamani, A.B. Mandal, G. Sekaran, Treatment of textile wastewater by homogeneous and heterogeneous fenton oxidation processes, Desalination, 281 (2011) 438–445.

[25] F. Zhang, J. Liu, I. IIvanov, M. Hatzell, W. Yang, Y. Ahn, B. Logan, Reference and counter electrode positions affect electrochemical characterization of bioanodes in different bioelectrochemical systems, Biotechnol. Bioeng., 111 (2014) 1931–1939.

[26] T.Z. Mahmoudabadi, F. Abbasi, M. Jalili, P. Talebi, Effectiveness of Plantago major extract as a natural coagulant in removal of Reactive Blue 19 dye from wastewater, Int. J. Environ. Sci. Technol., 16 (2019) 7893–7900.

[27] T.Z. Mahmoudabadi, P. Talebi, M. Jalili, Removing Disperse red 60 and Reactive Blue 19 dyes removal by using *Alcea rosea* root mucilage as a natural coagulant, AMB Express, 9 (2019) 113.

[28] H. Bel Hadjltaief, M.E. Galvez, M. Ben Zina, P. Da Costa, TiO_2/clay as a heterogeneous catalyst in photocatalytic/photochemical oxidation of anionic Reactive Blue 19, Arabian J. Chem., 12 (2019) 1454–1462.

[29] A. Rezaee, M.T. Ghaneian, S.J. Hashemian, G. Moussavi, A. Khavanin, G. Ghanizadeh, Decolorization of Reactive Blue 19 Dye from textile wastewater by the UV/H_2O_2 process, J. Appl. Sci., 8 (2008) 1108–1112.

[30] Ö. Erdem, N. Cihangir, Color removal of some textile dyes from aqueous solutions using *Trametes versicolor*, Hacettepe J. Biol. Chem., 45 (2017) 499–507.

[31] I. Sirés, E. Brillas, M. Oturan, M. Rodrigo, M. Panizza, Electrochemical advanced oxidation processes: today and tomorrow. A review, Environ. Sci. Pollut. Res. Int., 21 (2014) 8336–8367.

[32] M. Siddique, R. Farooq, Z.M. Khan, Z. Khan, S.F. Shaukat, Enhanced decomposition of Reactive Blue 19 dye in ultrasound-assisted electrochemical reactor, Ultrason. Sonochem., 18 (2011) 190–196.

[33] M. Collivignarelli, A. Abbà, M. Carnevale Miino, S. Damiani, Treatments for color removal from wastewater: state of the art, J. Environ. Manage., 236 (2019) 727–745.

[34] S. Sharma, J.P. Ruparelia, M.L. Patel, A General Review on Advanced Oxidation Processes for Waste Water Treatment, International Conference on Current Trends in Technology, Ahmedabad, Gujarat, 2011, pp. 1–7.

[35] A. Bedolla-Guzman, R. Feria-Reyes, S. Gutierrez-Granados, J.M. Peralta-Hernández, Decolorization and degradation of Reactive Yellow HF aqueous solutions by electrochemical advanced oxidation processes, Environ. Sci. Pollut. Res., 24 (2017) 12506–12514.

[36] P. Atkins, J. del Paula, Elements of Physical Chemistry, Oxford University Press, Oxford, 2013.